Transaction A: Civil Engineering
Vol. 16, No. 4, pp. 321–330

SCIENTIA IRANICA

Torsional Behaviour of High-Strength Concrete Beams Strengthened Using CFRP Sheets; an Experimental and Analytical Study

M.R. Mohammadizadeh[1,*] and M.J. Fadaee[1]

Abstract. *An experimental investigation of the strengthening of the torsional resistance of High-Strength Concrete (HSC) beams using Carbon-Fiber-Reinforced-Polymers (CFRP) is conducted. A total of seven beams are tested. Three beams are designated as reference specimens and four beams are strengthened using CFRP wrapping of different configuration and then tested. The variables considered in the experimental study include different wrap configurations such as: U-wrapping, full and strip wrapping, the effect of the number of CFRP plies and the influence of anchors in U-wrapped test beams. The reference and the strengthened beams are subjected to pure torsional moment. The load, the twist angle of the beams and the strains at longitudinal, transverse re-bars and CFRP are recorded to failure. In the current study, the ductility ratios and their increased percentage are investigated using two rather different methods. In further study, increasing the cracking, yield and ultimate torsional capacity of the strengthened beams is evaluated. Finally, experimental results are compared to several analytical results. The ultimate torsional strengths that are obtained by one of the analytical methods are in good agreement with the experimental results.*

Keywords: *Analytical; CFRP; Ductility; HSC; Strengthening; Twist; Torsion.*

INTRODUCTION

The repair and retrofitting of existing structures has become a major part of construction activity in many countries. To a large extent, this can be attributed to the aging of the infrastructure. Some of the structures are damaged by environmental effects, which include the corrosion of steel, variations in temperature and freeze-thaw cycles. There are always cases of construction-related and design-related deficiencies that need correction. Many structures, on the other hand, need strengthening because the allowable loads have increased or new codes have made the structures substandard. This last case applies mostly to seismic regions, where new standards are more stringent than the old.

1. *Department of Civil Engineering, Kerman University, P.O. Box 76169-14111, Kerman, Iran.*
*. *Corresponding author. E-mail: mrzmohammadizadeh@yahoo.com*

Received 23 May 2008; received in revised form 12 October 2008; accepted 1 November 2008

The method of strengthening structures with externally bonded Fiber-Reinforced-Polymer (FRP) composite material has received considerable attention because of its benefits in the last two decades. The advantages of composite materials in comparison with traditional construction materials such as steel wood and concrete are that they are non-corrosive, non-magnetic, resistant to various types of chemicals, of high strength and light-weight.

Studies concerning the strengthening of torsional members with FRP composites are very limited and meager data or design guidelines are available in the literature [1-12]. All of the studies conducted on torsional strengthening are related to normal strength concrete beams and practically no work has been carried out so far on high-strength concrete. The lack of experimental and analytical studies, along with the increasing interest in the use of FRP materials in the repair and rehabilitation of concrete structures, has led to the present research on the torsional behavior of high-strength concrete beams strengthened with CFRP sheets.

EXPERIMENTAL PROGRAM

Specimens Details

Seven rectangular beam specimens, having a cross section of 150 × 350 mm, were constructed in the laboratory and tested under pure torsion. The total length of the beams was 2000 mm and the length of the test region was approximately 1600 mm at the middle of the beams. Additional transverse reinforcement was placed at both ends of each specimen so that failure would occur in the central test region of the beam. The transverse and longitudinal reinforcements were arranged according to the design provisions of ACI [13]. The specimens were reinforced with four 14-mm diameter longitudinal bars located at four corners of the cross-section. Stirrups of 8 mm diameter were spaced at 80 mm on the center throughout the test region. The total steel ratio of longitudinal and transverse reinforcement was 2.13%. Three of the beams called REF1, REF2 and REF3 were tested without FRP as reference beams. The rest of the beams were then strengthened by carbon fiber (Mbrace CF 240) in different configurations. The CFRP sheets and epoxy resins were supplied by Master Builder's Technologies (MBT, 2003). The properties of the used fiber are shown in Table 1 [14].

In all strengthened beams, CFRP were employed vertically with respect to the longitudinal beam axis. One of the beams was wrapped by one layer of CFRP around the perimeter of the section and along the entire beam called CW1. Beam CW2 was wrapped by two layers of CFRP. Beam CUJ-anc. was wrapped by CFRP on two sides and also at the bottom as a U-jacket along the entire beam, and the free edges of CFRPs on the two sides were anchored to the top of the beam. Beam CS1 was wrapped by a 100 mm one layer strip of CFRP around the perimeter of the section at 100 mm spacing. The overlap length for the CFRP wrap was 15 cm. Table 2 shows the specifications of the specimen beams.

Material Properties

High strength concrete was designed for the 28-day cylinder compressive strength of 75 MPa and supplied by a local ready-mix plant. The actual concrete strength was considered as the average of at least six standard cube specimens of 100 × 100 × 100 mm converted to American cylinder specimen strength. The maximum size of coarse aggregate for the concrete was 10 mm. Both beams and cubes were kept under the same curing condition until testing.

The yield strengths of the transverse and longitudinal re-bars obtained from tensile tests were 397 MPa and 480 MPa, respectively.

Test Setup and Instrumentation

Details of the setup are shown in Figure 1. A 2-MN hydraulic jack was used to apply the load at the active support. The load had a 400 mm lever arm from the centroidal axis of the beam. A 2-MN compression load cell was used to measure the applied load. The hydraulic jack had a stroke length of 150 mm, providing a 35-degree twist capacity for the beam. A reaction arm was used at the passive support to balance the applied load by attaching the arm to the laboratory strong floor. The reaction arm had a 400 mm eccentricity from the centroidal axis

Table 1. Properties of fibers.

Type of Fiber	Thickness (mm)	Modulus of Elasticity (MPa)	Ultimate Tensile Strength (MPa)	Ultimate Tensile Elongation
CF 240	0.176	240,000	3800	1.55%

Table 2. The characteristics of the specimens.

Specimen	Configuration	No. of Layers	Using Anchorage	Concrete Compressive Strength MPa
REF1	Control beam	None	-	78.94
REF2	Control beam	None	-	77.82
REF3	Control beam	None	-	79.34
CS1	Full Strip	1	No	78.52
CUJ-anc.	U-jacket	1	Yes	80.56
CW1	Full wrap	1	No	79.12
CW2	Full wrap	2	No	74.95

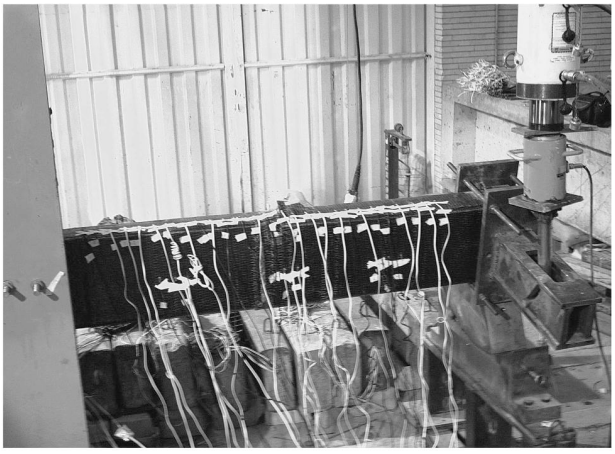

Figure 1. Test setup.

of the beam. After cracking, the beam elongates longitudinally. To avoid any longitudinal restraint and subsequent compression, the beam was allowed to slide and elongate freely. This was achieved by supporting the end of the beam on rollers at the passive support. The twist angle of the free end (the point of applying the torque) was measured by a clinometer.

In each beam, 12 strain gauges were used to measure strains on the reinforcing bars. Three strain gauges were mounted on three stirrups within the test region; one stirrup located at mid-span and two stirrups located symmetrically 400 mm away from the mid-span. Each stirrup was instrumented with one strain gauge, mounted at the middle of the long leg (side face; see Figure 2). Nine strain gauges were mounted on longitudinal bars at three different sections of the test region. One set of three gauges was located in the middle and the other two sets were symmetrically located 400 mm away from the middle on each side of the test beam. At each section, two gauges were mounted on the bottom corner bars and one gauge on the upper corner bar.

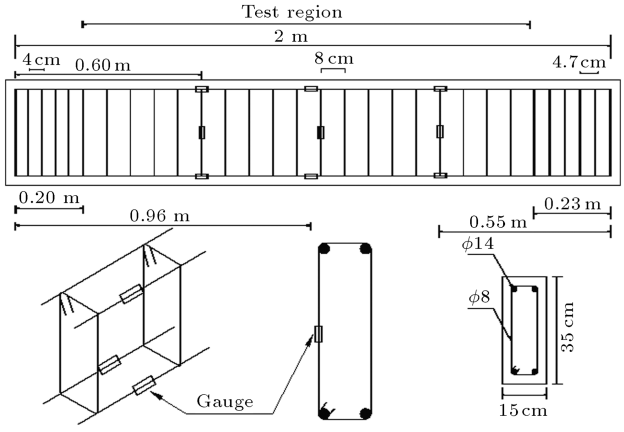

Figure 2. Location of strain gauges along the beam; strain gauges on stirrups and strain gauges on longitudinal bars.

For each strengthened beam, in addition to the instruments provided similar to the reference beams, at least 36 strain gauges were attached to the CFRP sheets on the middle part of one of its sides along the principal fiber direction with a spacing of 50 mm. These large numbers of strain gauges were used for the reason that the failure region along the entire length of the beam under pure torsion was unknown.

Test Procedure

Loads and strains measures were recorded through a computer-driven data acquisition system. Before testing, the cracking and ultimate strengths of the beam specimens were approximately estimated using the available analytical methods. Prior to the failure of the beam, data were recorded at a prescribed load increment. Smaller increments were applied around the cracking state to accurately measure the torque value closest to the actual cracking torque. The loading process was carried out as stress control. For the control beams, at every load stage after cracking, the load was held constant for several minutes before recording data after which the crack pattern was marked and the crack width and spacing were measured.

TEST RESULTS AND DISCUSSIONS

Behavior of the Strengthened Beams

The cracking and yield torques along with their percentage increase in comparison to the reference beams for all the strengthened beams are listed in Table 3.

For the three reference beams, cracking torque values are very close together. It can be seen that the cracking and yield torques of all strengthened beams are greater than those of the reference beams. An increase of 81.84% and an increase of 54.51% for cracking and yield torque, respectively, were recorded for CW2. The increasing magnitude depends on the CFRP reinforcement ratio and the strengthening configuration.

Table 4 indicates the results of the tests in terms of the ultimate torque and the twist angle (ϕ_{cr} and ϕ_P for cracking and ultimate torques, respectively) and the corresponding torque increase percentage and modes of failure for all 7 specimens. It can also be observed in Tables 3 and 4 that the cracking, yield and ultimate torque values of specimens CUJ-anc. and CW1 are approximately the same in spite of the fact that only three sides of the beam, CUJ-anc., are strengthened. It may be due to anchoring influence, which is much more effective than the strengthening configuration in this case. In fact, the anchors were used to eliminate the debonding or delamination of the CFRP jacket at its free edge. Furthermore, the loop

Table 3. Cracking and yielding torques obtained from experiments and corresponding increase percentage.

Specimen	Cracking Torque (KN.m)	Yield Torque (KN.m)	Cracking Torque Increasing (%)	Yield Torque Increasing (%)
REF1	8.30	14.20	-	-
REF2	9.51	15.00	-	-
REF3	9.58	18.00	-	-
CS1	12.25	16.70	34.22	6.14
CW1	16.46	22.50	80.33	43.01
CUJ-anc.	16.12	23.00	76.58	46.19
CW2	16.60	24.31	81.84	54.51

Table 4. Cracking twist angle, ultimate torques and corresponding twist angle of the beams.

Specimen	ϕ_{cr} Degrees	ϕ_P Degrees	$T_{n_{\max}}$ (KNm)	Ultimate Torque Increasing (%)	Mode of Failure
REF1	1.10	8.50	18.622	-	Yield & crushing
REF2	1.75	8.50	18.337	-	Yield & crushing
REF3	1.10	7.90	19.160	-	Yield & crushing
CS1	2.00	11.00	20.50	9.57	Debonding
CUJ-anc.	2.35	12.70	29.850	59.54	Rupture
CW1	2.50	11.90	29.480	57.56	Rupture
CW2	1.80	18.10	36.040	92.62	Rupture

of the force transferring mechanism provided by the composite sheets was completed by the bolts.

In Table 4, the percentage increase in the ultimate torques is based upon comparing the ultimate torques of the beams strengthened by CFRP with the average ultimate torque of the reference beams (specimens REF1, REF2 and REF3), which is equal to 18.71 KNm.

The torque-twist behavior of beams wrapped with CFRP sheets along with reference beams are plotted in Figure 3.

In this figure, curves are labeled with the specimens' codes. As expected, minor differences in the compressive strengths of the reference beams does not affect their behavior.

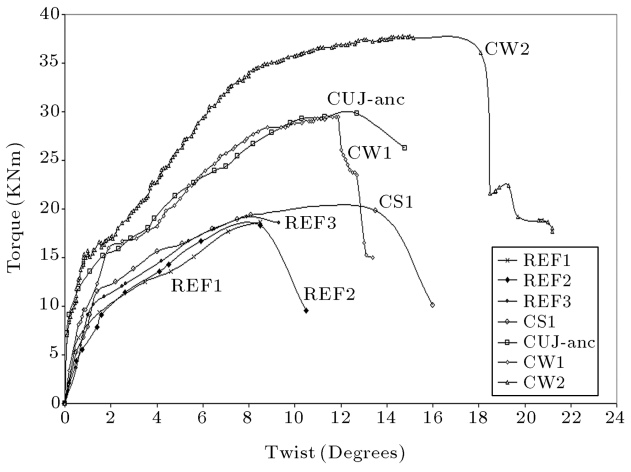

Figure 3. Torque-twist curves for all specimens.

In Figure 3, the difference observed in the initial stiffness of the beams can be attributed to the less-than-perfect fixed condition achieved in the setup. The authors believe that such a difference does not substantially affect the result of the torsional retrofitting of the specimens.

There are three different behavioral zones on each torque-twist curve as seen in Figure 3 qualitatively. The first zone represents the stiffness of the un-cracked beam, the second zone represents the stiffness of the cracked concrete beam strengthened with CFRP sheets and, finally, the third zone corresponds to a damaged beam with wide cracks, yielding torsional reinforcement and rupturing the composite material.

Figure 3 also exhibits that the complete wrap of the torsion region of a reinforced concrete beam is very effective in increasing the torsional strength of the beam, compared to a beam strengthened by one layer of strip. The reason for the deficiency of the strengthened beam, CS1, using strip rather than full wrap, is that the cracks occur between the strips and then are opened up. The completely wrapped specimens such as CW1 and CW2 do not show similar behavior because the cracks are not allowed to be opened due to the restraint provided by the fibers.

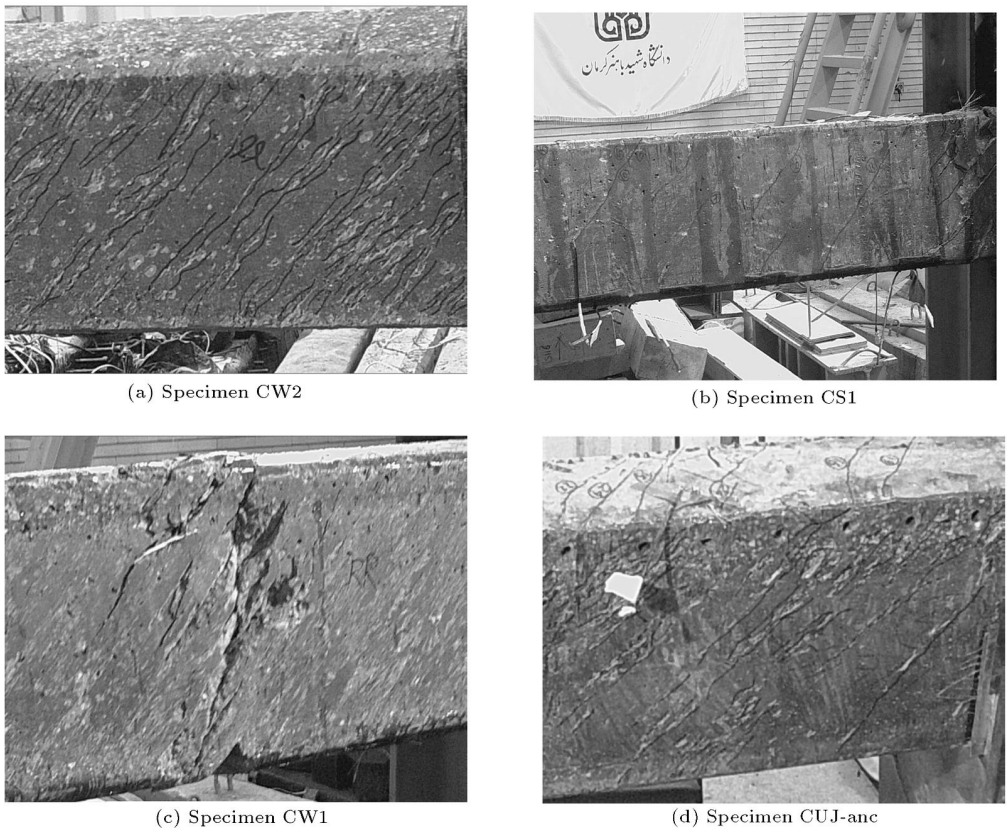

(a) Specimen CW2

(b) Specimen CS1

(c) Specimen CW1

(d) Specimen CUJ-anc

Figure 4. Crack distribution in the strengthened specimens.

Figure 4 exhibits crack distribution on one side of the strengthened specimens.

As indicated in Figure 5, the failure modes of all the strengthened beams are controlled by CFRP rupture at ultimate torque except beam CS1. This phenomenon is attributed to the configuration of CFRP wrapping in the strengthened beams, which is full (four-side) wrapping.

In beam CS1, after debonding, which occurs at the first CFRP strip overlap at the region close to the passive support, the cracks of that region will be opened causing the failure of the beam at a region close to the same support (see Figure 5a).

As can be seen in Figure 5b, after developing cracks in beam CW1, CFRP will be ruptured, followed by extensive concrete cracking, which ultimately results in the beam failure at a region close to its middle.

Beam CW2 sustains much more ultimate torque than the other strengthened beams because its entire perimeter was strengthened with more FRP layers. The specimen CW2 sustains an ultimate torsional moment of 92.62% more than the average ultimate torque of the reference beams. The failure of this beam occurs close to the passive support through the CFRP rupture (see Figure 5c).

The behavior of beam CUJ-anc. to the ultimate strength point is similar to beam CW1 and sustains ultimate torque very close to that of CW1. During loading, the cracks created on the top face of the beam (where it is not wrapped by CFRP) are gradually opened. The beam fails by CFRP rupture at a region close to the passive support where one of the cracks becomes the major crack (see Figure 5d).

Ductility

The ductility ratio, μ_ϕ, is usually defined as:

$$\mu_\phi = \frac{\phi_P}{\phi_Y}, \tag{1}$$

where ϕ_P is the twist angle at the ultimate torque and ϕ_Y is the yield twist angle. This ratio indirectly represents the amount of energy that a member can store during plastic deformations and so represents the ductility or energy absorbing capacity of the member. This concept of ductility can be applied to strengthened reinforced concrete members in a similar manner.

Some other researchers have proposed the following relation for computing the ductility ratio [15]:

$$\mu_{\phi,0.85P} = \frac{\phi_{0.85P}}{\phi_Y}, \tag{2}$$

where $\phi_{0.85P}$ is the twist angle at 85% of the peak torque beyond the peak point.

(a) Debonding of CFRP (specimen CS1)

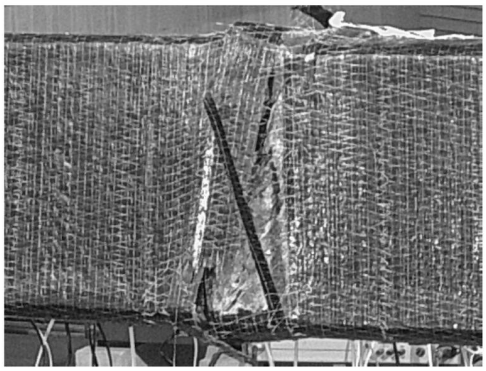

(b) Rupture of CFRP (specimen CW1)

(c) Rupture of CFRP (specimen CW2)

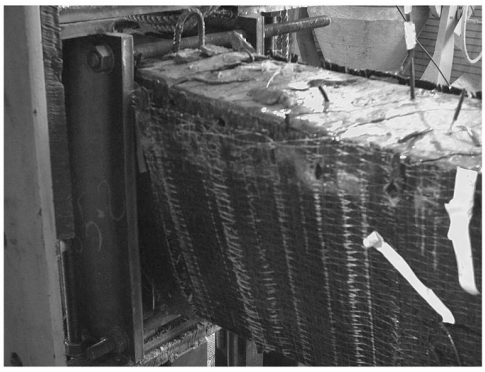

(d) Rupture of CFRP (specimen CUJ-anc)

Figure 5. Modes of failure of the strengthened beams.

Table 5. Comparison of specimens ductility ratios based on ϕ_P and $\phi_{0.85P}$.

Specimen	ϕ_y	ϕ_P	$\mu_{\phi,P} = \phi_P/\phi_y$	**Ductility Increasing, Equation 1 (%)**	$\phi_{0.85P}$	$\mu_{\phi,0.85P} = \phi_{0.85P}/\phi_y$	**Ductility Increasing, Equation 2 (%)**
REF1	5.15	8.50	1.65	-	-	-	-
REF2	4.70	8.50	1.81	-	9.40	1.72	-
REF3	6.50	7.90	1.22	-	-	-	-
CS1	5.40	11.00	2.04	30.77	14.50	2.69	56.12
CUJ-anc.	5.70	12.70	2.23	42.95	15.20	2.67	55.23
CW1	5.60	11.90	2.13	36.54	12.20	2.18	26.74
CW2	4.50	18.10	4.02	157.69	18.40	4.09	137.79

Ductility ratios are calculated for beams using both Equations 1 and 2 and then tabulated in Table 5.

In Table 5, ductility ratios of the strengthened beams resulted from Equations 1 and 2 are compared with the average ductility of the reference beams REF1, REF2 and REF3.

The maximum ductility ratio, μ_ϕ using Equations 1 and 2, belongs to beam CW2 with values of 4.02 and 4.09, respectively. These values show a 2.6 and 2.4 times increase in ductility compared with the average ductility of beams REF1, REF2 and REF3. The least increase in ductility is related to specimen CS1 with a value of 30.77%.

The percentage increase in the ductility of beams CUJ-anc. and CS1 based upon Equation 2 is higher than that of beam CW1. It may be due to the lower confinement of beams CUJ-anc. and CS1 compared to the beams strengthened by being completely CFRP wrapped. During loading, the number of cracks created along the entire top face of beam CUJ-anc. (where there is no CFRP wrapping) are smaller and their width are greater compared to the cracks created on the other three faces of the beam. For beam CS1, similar to

beam CUJ-anc., a smaller number of cracks of greater width occurred between strips, compared to the cracks that were created under strips. Therefore, unlike the beams that are strengthened along the entire length completely, a sudden decreasing in the load bearing capacity was not observed at the moment of CFRP rupture and the load descended evenly.

Experimental Data Analysis

Analytical methods for calculating the FRP contribution to the torsional capacity of strengthened beams are very limited. These methods are illustrated briefly in the following.

Analytical FIB-14 Method

One of these methods has come in [16] in which the results of the effective strain relating to the shear strengthened beams were used. In [16], the FRP contribution to torsional capacity, due to force couples that are created by a closed tube is considered. In this method, ultimate torque calculations are based upon the fiber orientation and the mode of failure. When the failure of the test beam is controlled by FRP rupture and the fiber orientation is vertical to the longitudinal axis, the contribution of FRP sheets to ultimate strength is determined using effective strain in the fibers. Effective strain in the fibers is determined using the empirical equations proposed in [16]. If the rupture of fibers is not the governing failure mode, a design approach based upon effective bond length is used to calculate the ultimate strength [17]. Thus, the FRP contribution to the torsional capacity based on the above is calculated as follows:

For complete wrap and strip:

$$T_{n_{frp}} = 2\varepsilon_{ke,f} E_{fu} \frac{t_f b_f}{s_f} A_c [\cot\alpha + \cot\beta] \sin\beta. \quad (3)$$

For U-wrap with anchors:

$$T_{n_{frp}} = \varepsilon_{ke,f} E_{fu} \frac{t_f b_f}{s_f} A_c [\cot\alpha + \cot\beta] \sin\beta, \quad (4)$$

where E_{fu} is the modulus of elasticity of FRP in the principal fiber orientation, t_f is the thickness of the FRP sheet, s_f is the center-to-center spacing of FRP strips, b_f is the minimum width of the cross section over the effective depth of the cross section, A_c is the gross sectional area of concrete, P_c is the circumference enclosing gross sectional area of the concrete, α is the angle of torsion crack and β is the angle of orientation of the fibers both measured from the member's longitudinal axis, and $\varepsilon_{ke,f}$ is the characteristic value of effective fiber strain, which is defined as:

$$\varepsilon_{fk,e} = K\varepsilon_{f,e} \le \varepsilon_{\max} = 5000\mu, \quad (5)$$

where K is the reduction ratio for defining the characteristic effective FRP strain.

For beams with a continuous jacket, terms b_f and s_f have identical values.

The corresponding equation to calculate the effective strain in FRP, $\varepsilon_{f,e}$, is available in [16].

Hii's method

The second method was presented by Hii et al. [8] in which in order to calculate the FRP contribution to the torsional capacity, the solid section under torsion was considered as an equivalent hollow tube.

The FRP contribution to the torsional capacity for a strengthened beam with complete wrap or strip is as follows:

$$T_{n_{frp}} = 2\varepsilon_{ke,f} E_{fu} \frac{t_f b_f}{s_f} (0.85 A_{oh}) [\cot\alpha + \cot\beta] \sin\beta, \quad (6)$$

where A_{oh} is the area enclosed by the outermost closed stirrups.

Combination of FIB-14 Method and FRP Strain Obtained from Experiments

The third method uses FIB-14's equations and the average effective strain obtained from the experiments.

In order to compare the effective strain obtained from the experiments with the calculated effective strain, the calculated effective strain, $\varepsilon_{f,\text{calc}}$, for each strengthened specimen is determined from the experimental FRP contribution to torsional torque, $T_{f,\text{exp}}$, by the following equation, which is resulted from Equation 3:

$$\varepsilon_{f,\text{calc}} = T_{f,\text{exp}} / \lfloor 2E_f b_f t_f s_f^{-1} A_c (\cot\alpha + \cot\beta) \sin\beta \rfloor, \quad (7)$$

where the experimental FRP contribution to torsional strength is determined by subtracting the ultimate torques of the reference beams, T_{ref}, from the ultimate torques of strengthened specimens, $T_{\text{exp}} (T_{f,\text{exp}} = T_{\text{exp}} - T_{\text{ref}})$.

Table 6 shows the effective, the characteristic effective and the average experimental effective strain values. The values in the first, second and last columns were obtained from FIB-14 and the recorded data at the peak torque, respectively. The average composite tensile strain recorded on the beam side is ranged between 1871μ and 4000μ, well below the composite ultimate strain of 1.55%.

In this study, three methods were used for calculating the torsional capacity due to the CFRP sheets.

It must be noted that the results of Equation 3 for specimen CUJ-anc. are very close to the experimental results, but surprisingly the CFRP contribution to the torsional strength of specimen CUJ-anc. obtained from experiments is twice the value resulted from

Table 6. Comparison of the average experimental effective strain with the effective strain obtained from corresponding equations.

Specimen	$\varepsilon_{f,e}(\mu\varepsilon)$	$\varepsilon_{fk,e}(\mu\varepsilon)$	$\varepsilon_{f,\text{calc}}(\mu\varepsilon)$	$\varepsilon_{f,\text{ave,exp}}(\mu\varepsilon)$
CS1	9932	5000	1019	4000
CUJ-anc.	9272	5000	2512	2508
CW1	8830	5000	2428	2666
CW2	7422	5000	1954	1871

Equation 4, which is recommended in the literature for such beams. Of course, more experiments are required to confirm this.

In Table 7, the results obtained from analytical methods are compared with experimental results. The results in Table 7 are based upon a 45° crack angle for all specimens.

From Table 7, it can be seen that the torsional contribution of CFRP estimated by FIB-14 is generally unconservative. The third column of Table 7 shows the results obtained by average experimental effective strains and the FIB-14 method. The results obtained by Hii's method are more conservative in comparison with the third method.

The ultimate torsional strength of beams strengthened by FRP can be obtained by adding the contribution of the fibers and that of the reinforced concrete beam, as follows:

$$T_n = T_{n_s} + T_{n_{frp}}. \tag{8}$$

Hence, the contribution to torsional strength of the reference beams considering ACI-Code provisions is calculated as follows [13].

$$T_{n_s} = \frac{2A_\circ A_t f_{yv}}{s}\cot(\alpha), \tag{9}$$

where, $A_\circ$ is the cross sectional area bounded by the center line of the shear flow, A_t is the area of one leg of the transverse steel reinforcement (stirrups), f_{yv} is the yield strength of the transverse steel reinforcement and s is the spacing of the stirrups.

Comparing the results of the second and third methods shows that the FIB-14 method based on average experimental effective strain is more realistic.

CONCLUSIONS

From analytical and experimental studies presented in this work, the following conclusions can be made.

The cracking and yield torques of all strengthened beams are greater than those of the reference beams. The increase in magnitude depends on the FRP reinforcement ratio and the strengthening configuration. An increase of 82% in cracking and an increase of 55% in the yield torque were recorded for beam CW2.

Adding anchors to the U jacket strengthening configuration is the reason why beam CUJ-anc. shows a torsional strength similar to that of beam CW1. This strengthening configuration (anchored FRP U-shape jacket) is important, because it is practical and can be used in retrofitting T-shape beams, which are simultaneously cast with the slabs.

Experimental results indicate that the estimation of the FRP contribution to torsional strength using the recommended equation in the literature is not true for the beams strengthened by anchored U-shape wrapping. It is found that using the equation available for full or strip wrapped specimens provides good results for such beams.

Comparing the ductility ratio of specimen CUJ-anc. with specimen CW1, a ductility increase percentage of 5% and 22% (using Equations 1 and 2, respectively) relating to CUJ-anc. is observed.

The largest ductility ratio is related to CW2 with an average value of 4.06 among all strengthened beams. This value shows about a 2.5 times increase in ductility when compared with the average ductility of the reference beams.

The best performing wrapping mechanism (as for the ductility) is full wrapping along the entire length

Table 7. Comparison of experimental and analytical ultimate torques.

	$T_{f,\text{exp}}/T_{n,frp}$	$T_{f,\text{exp}}/T_{n,frp}$	$T_{f,\text{exp}}/T_{n,frp}$	T_{exp}/T_n	T_{exp}/T_n	T_{exp}/T_n
Specimen	**FIB-14**	**Hii's Method**	**FIB-14** $\varepsilon_{f,\text{ave,exp}}(\mu\varepsilon)$	**FIB-14**	**Hii's Method**	**FIB-14** $\varepsilon_{f,\text{ave,exp}}(\mu\varepsilon)$
CS1	0.20	0.47	0.38	0.95	1.12	1.00
CUJ-anc.	0.50	1.16	1.00	0.80	1.19	1.13
CW1	0.49	1.12	0.91	0.79	1.18	1.08
CW2	0.39	0.90	1.04	0.60	1.04	1.13

with two layers of CFRP. The torsional strength of the retrofitted beam exceeded the value of the reference beams by up to 92.62%.

Comparing the results of the second and third methods indicates that the use of relationships corresponding to FIB-14's effective strain (that is, based upon the experimental shear strengthening data of beams), in order to estimate the torsional capacity of the retrofitted beams, is viable but new equations are required to assess the strains based upon statistical data corresponding to the experimental torsional strengthening.

NOMENCLATURE

$A_\circ$	cross sectional area bounded by the center line of the shear flow
$A_{\circ h}$	area enclosed by the outermost closed stirrups
A_c	gross sectional area of concrete
A_t	area of one leg of the transverse steel reinforcement (stirrups)
b_f	minimum width of the cross section over the effective depth of the cross section
E_{fu}	modulus of elasticity of FRP in the principal fiber orientation
f_{yv}	yield strength of the transverse steel reinforcement
K	reduction ratio for defining the characteristic effective FRP strain
P_c	circumference enclosing gross sectional area of concrete
s	spacing of the stirrups
s_f	center-to-center spacing of FRP strips
t_f	thickness of the FRP sheet
$T_{f,\text{exp}}$	experimental FRP contribution to torsional torque
T_{exp}	experimental ultimate torque of the FRP strengthened beam
T_n	nominal torsional capacity of the FRP strengthened beam
T_{n_s}	nominal torsional capacity due to steel reinforcement
$T_{n_{frp}}$	nominal torsional capacity due to FRP reinforcement
T_{ref}	ultimate torque of the reference beam (beam without FRP)
α	angle of torsion crack, with respect to the member's longitudinal axis
β	angle of orientation of the fibers, with respect to the member's longitudinal axis
$\varepsilon_{f,\text{calc}}$	calculated effective strain
$\varepsilon_{f,e}$	effective FRP strain
$\varepsilon_{ke,f}$	characteristic value of effective fiber strain
μ_ϕ	ductility ratio
$\mu_{\phi,0.85P}$	ductility ratio using twist angle at 85% of the peak torque beyond the peak point
ϕ_Y	twist angle at the yield torque
ϕ_P	twist angle at the ultimate torque
$\phi_{0.85P}$	twist angle at 85% of the peak torque beyond the peak point

REFERENCES

1. Ameli, M., Ronagh, H.R. and Dux, P.F. "Experimental investigations on FRP strengthening of beams in torsion", *FRP Compos. Civ. Eng.*, CICE 2004, Adelaide, Australia, pp. 587-592 (2004).
2. Ameli, M., Ronagh, H.R. and Dux, P.F. "Behaviour of FRP strengthened reinforced concrete beams under torsion", *ASCE, J. Compos. Constr.*, **11**(2), pp. 192-200 (2007).
3. Ghobarah, A., Ghorbel, M.N. and Chidiac, S.E. "Upgrading torsional resistance of reinforced concrete beams using fibre-reinforced polymer", *ASCE, J. Compos. Const.*, **6**(4), pp. 257-263 (2002).
4. Gosbell, T. and Meggs, R. "West gate bridge approach spans FRP strengthening Melbourne", *Australia. IABSE Sympo. Melbourne*, Melbourne, Australia (2002).
5. Hii, A.K.Y. and Al-Mahaidi, R. "Torsional strengthening of reinforced concrete beams using CFRP composites", *FRP Compos. Civ. Eng.*, CICE 2004, Adelaide, Australia, pp. 551-559 (2004).
6. Hii, A.K.Y. and Al-Mahaidi, R. "Torsional strengthening of solid and box-section RC beams using CFRP composites", *Compos. Constr. 2005 - 3rd Int. Conf.*, Lyon, France, pp. 59-68 (2005).
7. Hii, A.K.Y. and Al-Mahaidi, R. "Experimental investigation on torsional behaviour of solid and box-section reinforced concrete beams strengthened with carbon FRP using photogrammetry", *ASCE, J. Compos. Constr.*, **10**(4), pp. 321-329 (2006).
8. Hii, A.K.Y. and Al-Mahaidi, R. "Torsional capacity of CFRP strengthened reinforced concrete beams", *ASCE, J. Compos. Constr.*, **11**(1), pp. 71-80 (2007).
9. Panchacharam, S. and Belarbi, A. "Torsional behaviour of reinforced concrete beams strengthened with FRP composites", *FIB Congr.*, Osaka Japan (2002).
10. Ronagh, H.R. and Dux, P.F. "Full-scale torsion testing of concrete beams strengthened with CFRP", *Proc. 1st Int. Conf. Perform. Constr. Mater., in the New Millenium*, February, Cario, pp. 735-745 (2003).

11. Salom, P.R., Gergely, J. and Young, D.T. "Torsional strengthening of spandrel beams with fibre-reinforced polymer laminates", *ASCE, J. Compos. Constr.*, **8**(2), pp. 157-162 (2004).

12. Zhang, J.W., Lu, Z.T. and Zhu, H. "Experimental study on the behaviour of RC torsional members externally bonded with CFRP", *FRP Compos. Civ. Eng.*, **1**, pp. 713-722 (2001).

13. ACI 318-05 "Building code requirements for structural concrete", *Amer. Concr. Inst.*, Farmington Hills, MI (2005).

14. MBT. MBrace Brochure [online], http://www.mbtaus .com.au (2003).

15. Fang, I.K. and Shiau, J.K. "Torsional behaviour of normal-and high-strength concrete beams", *ACI Struct. J.*, **101**(3), pp. 304-313 (2004).

16. FIB (CEB-FIB) "Externally bonded FRP reinforcement for RC structures", *FIB Bulletin 14. FIB - Int. Fed. Struct. Concr.*, Lausanne, pp. 59-68 (2001).

17. Khalifa, A., Gold, W.J., Nanni, A. and Aziz, A. "Contribution of externally bonded FRP to shear capacity of flexural members", *ASCE, J. Compos. Constr.*, **2**(4), pp. 195-203 (1998).